STRUCTURAL CONTROLS ON FLUID FLOW AT THE ONEMANA AREA, COROMANDEL PENINSULA, NEW ZEALAND

Mariana Zuquim[1] and Julie Rowland[1]

[1] School of Environment, The University of Auckland, Private Bag 92019, Auckland, New Zealand.

mzuq901@aucklanduni.ac.nz

Keywords: *Onemana, paleo-geothermal system, structural controls, fluid flow, Coromandel Peninsula.*

ABSTRACT

The Onemana area, which lies at the eastern coast of the Coromandel Peninsula of New Zealand, is part of a broad NNE-trending corridor of epithermal Au-Ag deposits that runs from Tui mine in the southwest to Onemana/Ohui in the northeast. Silicified and altered rhyolitic flow banded rocks of the Whitianga Group and minor Coromandel Group andesites outcrop in the area. High-level silicification and quartz-kaolinite-type alteration follows a 3.5 km long and 1.8 km wide NE-SW trending aeromagnetic low/resistivity high which is delimitated to southeast by the NE-striking Whitipirorua fault. Veins and hydrothermal breccias are also confined to this alteration corridor. The paleo-geothermal system was present in the hanging wall of the Whitipirorua fault. At this fault block occurs a 260 m deep body of lacustrine sediments with hydrothermal eruption breccias and, possibly, sinters associated. Extensional fracturing is the main rock failure mechanism and dictates the structural permeability style at Onemana. Extensional veins and hydrothermal breccias strike N-S to NE, which are the main structural trends of the area, and could be linked with faults at depth, where shear failure is favoured. Flow banding exerted some control on fluid flow either through its primary permeability or by controlling fracture formation. The lower tensile strength orthogonal to the flow banding coupled with low overburden stress control fracture aperture, in a process facilitated by hydrostatic to supra-hydrostatic fluid pressure. As a result, vertically and sub-horizontally dipping hydrothermal breccias and veins trending parallel to the rock fabric are formed where the flow banding dips steeply and gently, respectively. The formation of highly silicified rock layers results from fluid circulation along porous rock beds, e.g., a spherulitic rhyolite flow.

1. GEOLOGICAL SETTING

The Onemana area lies at the east coast of Coromandel Peninsula (New Zealand), at the northeast end of the Karangahake-Ohui structural corridor (KOST). The KOST runs from Te Aroha, to the southwest, to Pauanui, to the northeast and consists of a NNE-trending, 50 km long by 7 km wide zone of intense hydrothermal alteration (Irvine and Smith, 1990, Rabone, 1991). Within the KOST, N- to NE-striking Au-Ag mineralised epithermal quartz veins were formed in association with NNE- to NE-striking controlling faults. Mineral exploration (drilling, mapping, geophysics, and geochemistry) was carried out at Onemana intermittently since 1970's (MacNamara, 1972; Maxwell, 1980), but no economically feasible resource has been delimitated to date.

The geology of Onemana consists of rhyolitic pyroclastic rocks and lavas of the Whitianga Group (Late Miocene to Pliocene) and dacitic to andesitic flows and plugs of the Coromandel Group (Miocene; Stevens and Boswell, 2006a). These units host veins and hydrothermal breccias formed by late stage hydrothermal activity (Fig. 1) and were also affected by high-level silicification and quartz-kaolinite-type alteration. The type of alteration was interpreted as the upper acid leached levels of the hydrothermal system (Robson, 1992).

A shallow epithermal system is suggested due to the presence of a 260 m deep body of lacustrine sediments associated with hydrothermal eruption breccias and sinters (Aldrich, 1995, Robson, 1992), the alteration type and colloform-banded chalcedony as the main vein fill material (Fig. 4D, F, G and H). A paleodepth of approximately 200 mVD is estimated for the outcrops of the costal sections of the area given that the lake sediments and sinters are indicative of near-paleosurface environment.

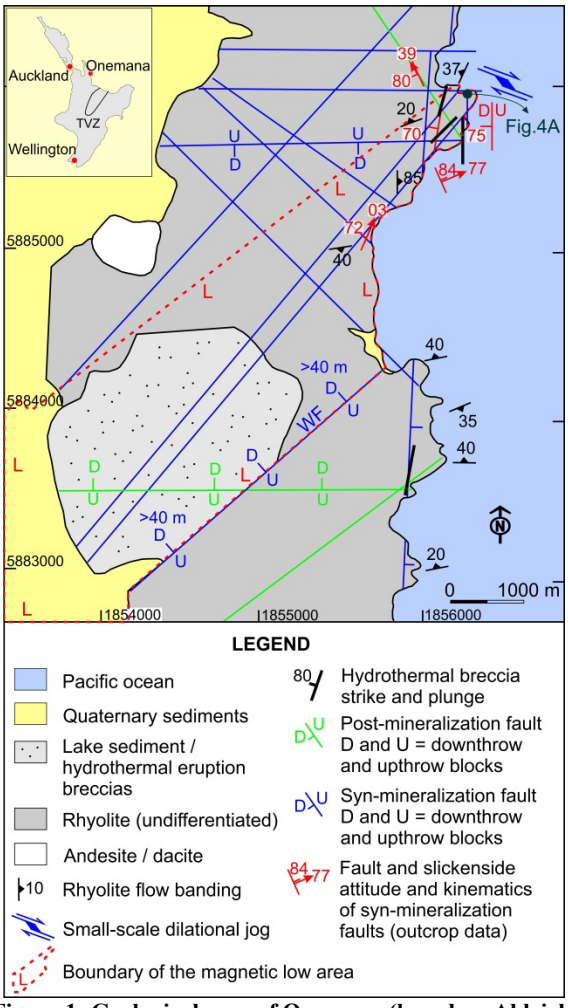

Figure 1: Geological map of Onemana (based on Aldrich, 1995 and Zuquim unpublished data). TVZ = Taupo Volcanic Zone; WF = Whitipirorua fault. Low magnetic zone boundary after Vidanovich (1991).

1.1 Structure

Faults and tectonic fractures at Onemana were formed by regional NW-SE extension and, possibly, by subsequent E-W extension (Zuquim, 2013 – in press). These paleostress fields imposed a predominantly normal displacement to the N-to-NE-striking faults, and a predominantly strike-slip displacement for the faults trending NW (Robson, 1992; Zuquim unpublished data). Slickensided fault planes with variable rakes were measured and plotted in the geological map (Fig. 1), but there is insufficient data to rigorously constrain the kinematics of the faults throughout the area due to the poor exposures away from the coastal cliffs. A small-scale dilational jog was observed within a NW-striking vein (Fig. 4C). Syn-mineralisation faults strike N-S, NE-SW, NW-SE and E-W, and closely-spaced extension fractures/veins are formed parallel to fault trace. The N- and NE-striking faults are the structures more closely associated with the formation of hydrothermal breccias and veins (Zuquim, unpublished data).

Hydrothermal alteration follows a 3.5 km long and 1.8 km wide NE-SW trending corridor which matches with an aeromagnetic low/resistivity high zone (Vidanovich, 1991; Vidanovich, 1995). N-striking aeromagnetic and resistivity anomalies, partially tested by drilling, transect this alteration corridor (Vidanovich, 1995). The alteration zone is delimitated to southeast by the NE-striking Whitipirorua fault and, possibly, to the northwest, by the NE-striking Pokohino fault (Robson, 1992). The paleo-geothermal system is in the hanging wall of the Whitipirorua fault (Fig. 1) and very little veining occurs at the footwall. The Whitipirorua fault neither crops out nor was intercepted by drilling to date, but extensional fractures were observed parallel to the fault trace (Zuquim unpublished data). Drilling at the hanging wall of the fault intercepted rhyolitic lavas beneath the lake sediments/hydrothermal eruption breccias at about 50 m.a.s.l. (Robson, 1992). At the footwall of the fault, rhyolites crop out at 90-100 m.a.s.l., indicating a minimum downthrown of 40-50 m to north for the Whitipirorua fault (Aldrich, 1995).

2. STRUCTURAL CONTROLS ON FLUID FLOW

In addition to the widespread hydrothermal alteration that affects the rhyolites in the area, hydrothermal fluid circulation is evinced by veins and several tabular bodies of hydrothermal breccias up to 2 m wide (Fig. 5A). The contact between these bodies and the host rock is sharp (Fig. 5A); rhyolite flow clasts within the breccia are 1-50 cm long and show variable rounding degree (Fig. 5A vs. Fig 5 B) and the matrix consists of vuggy chalcedony. Structurally controlled fluid flow at the Onemana paleodepth (200 mVD) occurred mainly within these hydrothermal breccias. A mechanical treatment for the development of the veins and hydrothermal breccias is given in the following section. These structures strike parallel to the fault zones and dip vertically (Fig. 1).

A permeability network is formed in zones of intersections of faults with different orientation due to the development of several intersecting fracture sets (e.g., Fig. 4A – dark green annotation). Most of the fractures are up to three cm thick, have a chalcedonic lining but do not show evidences of multiple crack-seal events.

2.1 Rock failure

Rheological and permeability parameters of the rhyolite flow, as well as how these parameters change throughout the lifespan of the hydrothermal system, were estimated based on data from some active and fossil geothermal systems of the Taupo Volcanic Zone (Table 1). Rowland and Simmons (2012) modeled the rock failure modes in an extensional tectonic setting using typical values for rhyolites and greywacke basement of the TVZ for 200 m depth (Fig. 2). Refer to Rowland and Simmons (2012) for failure criteria equations.

Table 1: Estimated mechanic and hydraulic parameters of rhyolite flow and how these parameters change through time.

Rhyolite flow	PRE-HYDROTHERMAL ACTIVITY	SYN-HYDROTHERMAL ACTIVITY
Bulk-rock permeability	$\geq 10^{-16}$ m^2 (1)	$< 10^{-16}$ m^2 (1)
Tensile strength[3]	≤ 10 MPa (1) 5 MPa to 13 MPa (2)	10 MPa? (1)
Density	≤ 2,200 kg/m^3	2.200 kg/m^3
P_f	Steady-state Hydrostatic	"Quasi" steady-state Hydrostatic to supra-hydrostatic
Main fluid flow pathway	-	Fault, fractures and bedding

[1] Based on Rowland and Simmons (2012). Permeability estimation is based on the concept that 10^{-16} m^2 is the threshold value required for convection; bulk permeabilities lower than 10^{-16} m^2 generates forced overpressures and rock failure (Rowland and Simmons, 2012).
[2] Based on Jackson et al. (1995)
[3] Long term values can be only a fraction of the laboratory-determined values (Sibson, 1998)

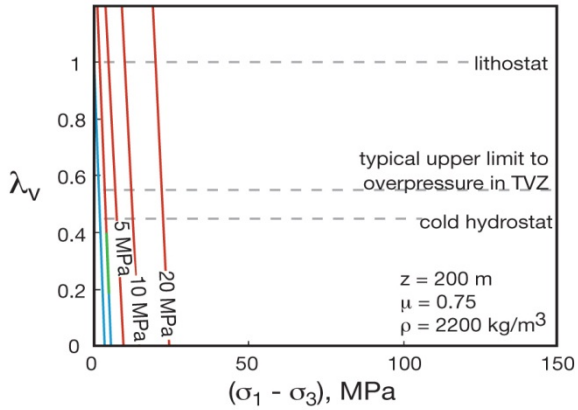

Figure 2: Failure mode diagram for extensional tectonic settings at 200 m depth (z). Failure modes: red = extensional, green = extensional-shear, blue = shear. Failure curves for rocks with tensile strength of 1, 5, 10 and 20 MPa and for reactivation of a cohesionless, pre-existing fault, optimally oriented for reactivation in relation to a vertical maximum compressive stress (σ_1). Coefficient of internal friction (μ) = 0.75 and density (ρ) = 2,200 kg/m^3. (σ_1- σ_3) = differential stress; Pore fluid factor (λ_v) = $\frac{P_f}{\sigma_v}$, where $\sigma_v = \sigma_1$ (after Rowland and Simmons, 2012).

Silicification is widespread at Onemana rhyolites and particularly well developed at the spherulitic units (Fig. 4E). The silicification process, also called as silica flooding, has profound implications for the mechanical and hydrological proprieties of the rocks. The depth in which purely extensional fracturing failure mode transitions to shear failure increases with the increment of the pore fluid factor (λ_v) and of the tensile strength of the rock (Sibson, 2000). Silicification increases the rock tensile strength and causes pore and fracture clogging (Sibson, 1998), leading to local slightly overpressured systems (λ_v slightly greater than 0.4), favouring extensional fracturing until greater depths.

The pore and fracture clogging caused by silicification initially decrease the rock permeability, but subsequently favours secondary permeability development by promoting fluid assisted rock failure. For pore fluid factors (λ_v) from 0.4 to 0.6, which is the typical range for epithermal environments (Rowland and Simmons, 2012), the main failure mechanism is pure extension (Fig. 2). An exception to extensional failure occurs for very weak rocks (<1 MPa) and for a cohesionless pre-existing fault optimally oriented for reactivation in relation to the stress field, which will undergo shear failure (Rowland and Simmons, 2012). It is not surprisingly that the most outstanding structural lineaments within satellite images and aerial photos at Onemana correspond in the field to persistent and closely spaced extensional fractures and very seldom to faults. It is likely that, at greater depths, these purely extensional structures are connected to faults, formed due to the greater differential stress at depth (Sibson, 2000; Cox, 2010).

Where present, faults show multiple stages of activation and fluid circulation. These multiple episodes are evinced by the formation of tectonic breccias in which the clasts consist of rhyolite and vein fragments (Fig. 5H and I). Veins occur at the interface of the fault breccia and the host rock.

While most of the extensional fractures are up to a few centimeters wide, some extensional fractures reach greater widths (10's cm). Most of these wider veins show a central cavity and are colloform-banded (Fig. 4B), evincing that they were formed by a series of crack-seal events. Some of the narrower banded veins are not symmetric on the walls (Fig. 4G), suggesting that that the interface between vein and host rock was the mechanically weaker surface, and that, probably, the vein did not have a central cavity.

3. FLOW BANDING CONTROLS ON FLUID FLOW - ORIENTATION, PERMEABILITY AND MECHANICAL PROPRIETIES

In addition to the secondary permeability of the rock dictated by extensional veins/fractures and hydrothermal breccias, the flow banding promoted vertical and (sub)horizontal permeability, depending on the flow banding dip.

Highly silicified horizons, notably the spherulitic unit, occurs in zones of moderate to shallow dipping flow banding (Fig. 5C). These silicified horizons are developed due to the greater primary permeability of some rock layers in relation to the adjacent beds. Secondary (sub)horizontal permeability is particularly promoted by the development of "stratabound" hydrothermal breccias on gently dipping rhyolite beds (Fig. 5D and G). At Onemana, these hydrothermal breccias show nil or very little clast rotation, and it is still possible to identify the mesh of vertical to subvertical fractures that allowed fluids to move through the rhyolite bed. Stratabound fractures in sedimentary rocks are fractures confined to layers that have a more brittle mechanical response to deformation than the adjacent beds. These fractures do not propagate into the adjacent beds. Fracture spacing is smaller in thinner layers and layers with lower tensile strength (Ladeira and Price, 1991; Schöpfer et al., 2011) and decreases with increasing overburden pressure and decreasing tensile strength until fracture saturation is reached (Schöpfer et al., 2011). At Onemana, not only these factors have influenced the formation of the fractures that evolved to "stratabound" hydrothermal breccias, but also a feedback between layer permeability and rock failure. More permeable layers can "leak" the fluids and avoid the pore-pressure build-up and the subsequent reduction of the effective stresses which can lead to hydraulic fracturing (Fig. 3 – blue circle). Less permeable layers (Fig. 3 – red circle) will be subjected to a greater fluid pressure increase and will undergo hydraulic fracturing first (Cosgrove, 1995).

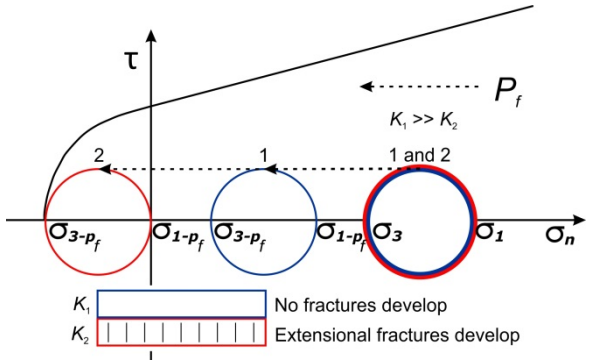

Figure 3: Influence of permeability (*K*) on hydraulic fracturing in layered rock. Initial stress state shown on overlapping red and blue circles; effective stress state shown on separate circles. Rectangles show the expression of changes in the effective stresses on a layered rock due to an increase of fluid pressure. Normal stress (σ_n) Vs. shear stress (τ) space. σ_1 and σ_3 = maximum and minimum stresses; P_f = fluid pressure (based on Cosgrove, 1995).

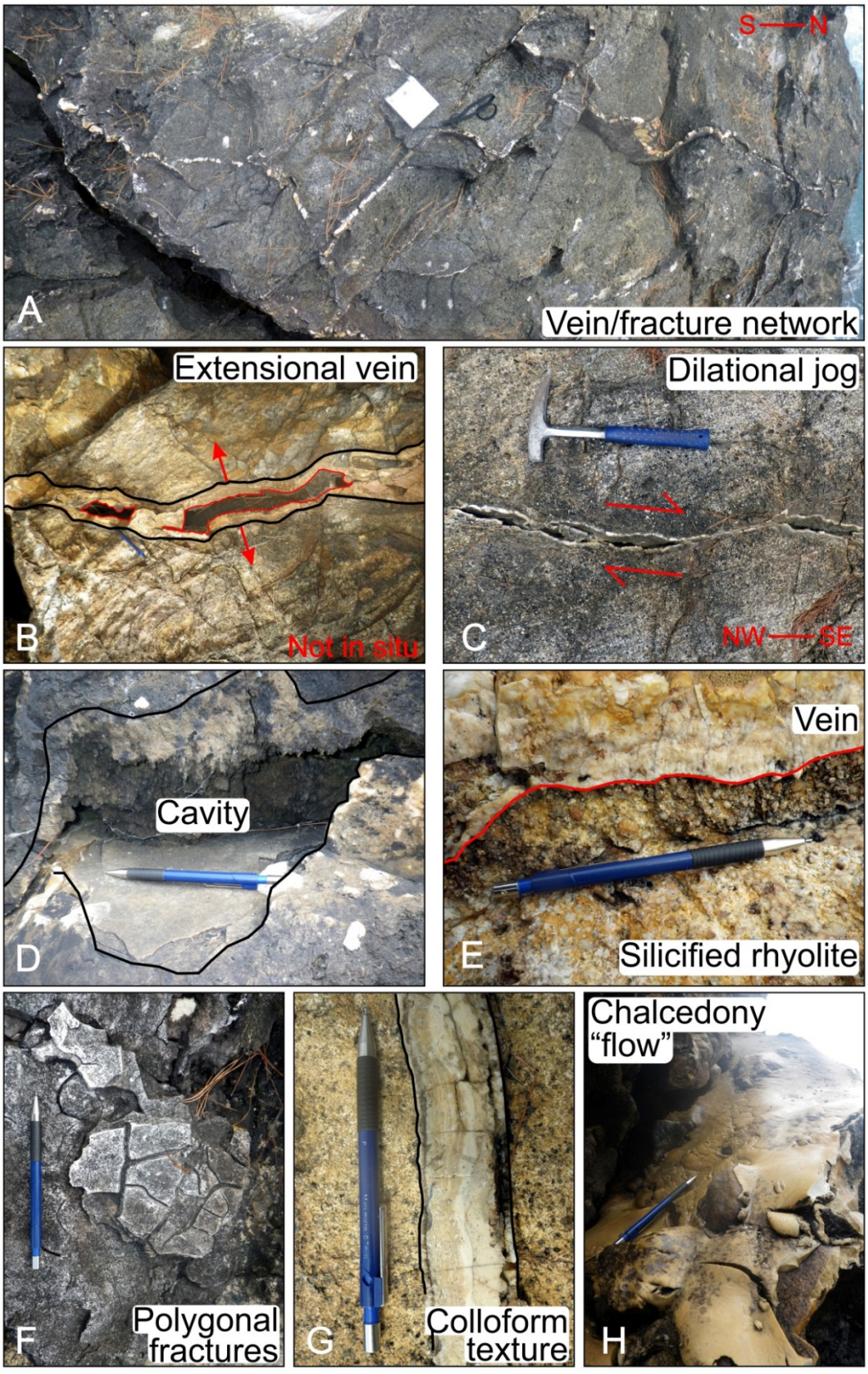

Figure 4: A. Vein network in zone of fault intersection (yellow dot at Fig.1). B. Extensional vein with central vug and irregular walls. C. Small-scale dilational jog. D. Cavity within host rock. Silica saturated fluids precipitate from the top and forms a blanket of chalcedony at the bottom. E. Interface quartz vein/spherulitic rhyolite. Rhyolite intensely silicified. F. polygonal fractures on chalcedony vein, formed by thermal contraction during solidification (Jébrak, 1997). G. Asymmetric banded vein, no central cavity. H. Surface of a fracture covered with a layer of chalcedony. Tension fractures and bulges in the layer suggest a brittle/plastic behavior during solidification.

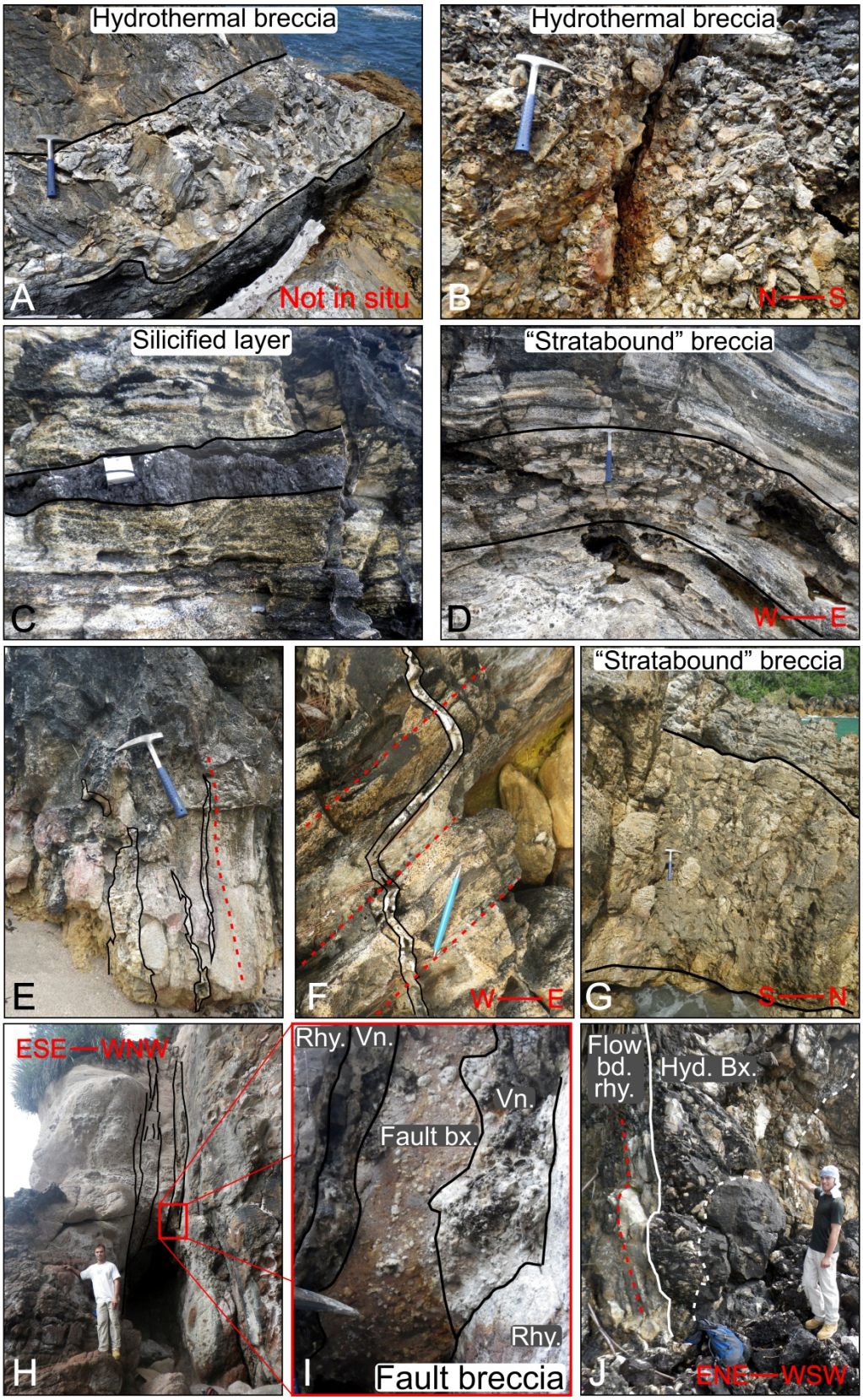

Figure 5: A. Tabular hydrothermal breccia. Misoriented angular clasts of rhyolite flow. B. Hydrothermal breccia (N-S/65°W). Rounded clasts, vuggy chalcedonic matrix. C. Silicified layer within rhyolite flow. Compass (scale) 6 cm wide. D. Hydrothermal breccia confined to a 0.5 m thick flow banded rhyolite layer. E. Extensional veins parallel to flow banding (dashed red line). F. Extensional veins crosscutting and refracting at flow banding (dashed red line). G. Hydrothermal breccia confined to a 2 m thick flow band layer. No clast rotation. H. Fault zone (N-S/80°E). Extensional veins (black lines). I. Vein clasts within fault breccia. J. Hydrothermal breccia parallel to flow banding (dashed red line). Sharp contact to east, transitional contact to west.

Veins and hydrothermal breccias oriented parallel to flow banding occur predominantly where the rock fabric dips steeply (Fig. 4E). These hydrothermal breccias show either sharp or gradational contact with the host rock (Fig. 5J). As discussed before, the majority of the outcrops of the Onemana area are estimated at < 200 mVD paleodepth. At Rotokawa geothermal field (Taupo Volcanic Zone of New Zealand), a differential stress of about 2-3 MPa was estimated at 200 mVD depth, based on vertical overburden stress calculated using rock density of 2.7 g/cm^3 and minimum horizontal stress data from fracture closure pressure of leak-off test (Davidson et al., 2012). Considering this very low differential stress conditions, different tensile strengths orthogonal and parallel to the rock fabric can determine the orientation of the fracture aperture, as demonstrated in Fig. 6. The presence of veins parallel to flow banding in Onemana suggests that the tensile strength orthogonal to the flow banding is equal or lower than the tensile strength parallel to bedding, as expected for layered rocks (Hoek, 1964). It is also suggested that circulating hydrothermal fluids act as to weaken the rhyolite and assisted rock failure by reducing the effective stress. Mechanical tests on anisotropic (layered) rocks show that the tensile strength orthogonal to the rock fabric is up to 4-5 times lower than parallel to the anisotropic plane (Nova and Zaninetti, 1990; Chen and Hsu, 2001). This control of flow banding orientation on rock failure also explains the formation of some unusual low angle extensional veins oriented parallel to the rhyolite flow banding that occur in the area (Fig. 6D).

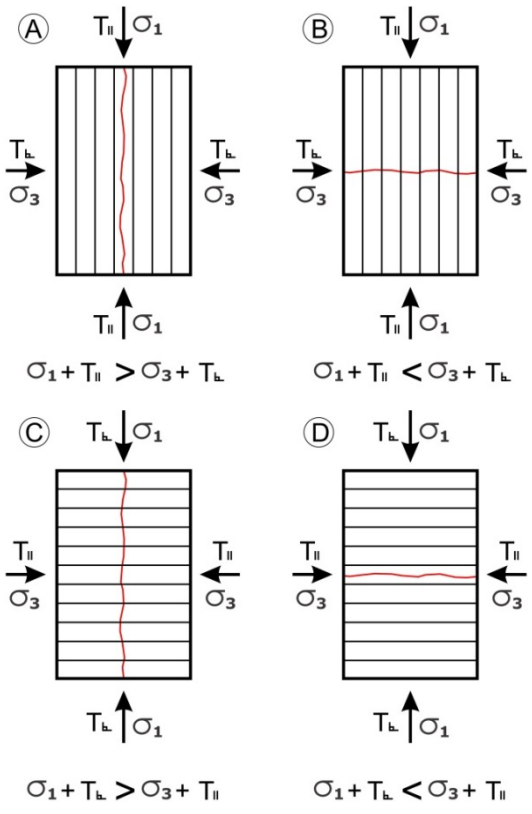

Figure 6: Controls of the different tensile strengths parallel and orthogonal to rock fabric and of the maximum and minimum stresses on the orientation of tensile fractures (based on Hudson and Harrison, 1997 and Cosgrove, 1995).

4. CONCLUSION

Field observation of the characteristics of the veins and hydrothermal breccias at the Onemana area gives insights of the mechanisms in which fluids percolate through the primary (connected pores) and secondary (fractures and faults) permeability within flow banded rhyolites at about 200 mVD paleodepth. Extensional fracturing is the predominant rock failure mode in the area and dictates the structural permeability style. Pervasive silicification plays an important role by causing pore clogging and allowing fluids to focus on structures instead of percolating throughout the rock primary permeability (Sibson, 2001).

Structurally controlled tabular bodies of hydrothermal breccia mirrors the faults of the area and are responsible for creating vertical permeability within the hydrothermal system. These hydrothermal breccias dip vertically or sub-vertically and can be up to 2 m wide. These tabular bodies are formed in zones of intense fracturing and may be linked with faults at depth, where shear failure is favoured (Sibson, 2001; Rowland and Simmons, 2012). Other hydrothermal breccias and veins are not related to any tectonic structure and are formed parallel to flow banding in zones where the rock fabric dips steeply. This local-scale structural setting suggests that the lower tensile strength perpendicular to the flow banding controls fracture aperture in a process facilitated by fluid-assisted rock failure.

Horizontally-directed primary and secondary permeability is promoted particularly where flow banding dips gently. The difference in the permeability of some rhyolite layers promotes different degrees of silicification throughout the rhyolitic sequence. “Stratabound” hydrothermal breccias, on the other hand, promote even greater horizontal permeability by highly disrupting the rhyolite beds and, consequently, creating sub-horizontal tabular bodies of hydrothermal breccia. These bodies are confined to up to few meters wide rock layers and have no apparent vertical connection with other beds. Feedback between layer permeability and rock failure may have caused a selected disruption at some rock beds. Less permeable layers will be subjected to a greater fluid pressure increase and will undergo hydraulic fracturing first. Conversely, more permeable layers can “leak” the fluids, thus avoiding the pore-pressure build-up and the subsequent hydraulic fracturing.

ACKNOWLEDGEMENTS

This research was largely funded through the MBIE Mineral Wealth of New Zealand program. Newmont Waihi Gold supported this research through provision of logistical support and data. We thank the land owners for allowing access to the mapped areas.

REFERENCES

Aldrich, S. M. *Volcanic geology and hydrothermal alteration of the Onemana Peninsula.* MSc thesis (unpublished), University of Waikato, Hamilton (1995).

Chen, C. S. and Hsu, S. C. Measurement of Indirect Tensile Strength of Anisotropic Rocks by the Ring Test. *Rock Mechanics and Rock Engineering,* 34**,** 293-321 (2001).

Cosgrove, J. W. The expression of hydraulic fracturing in rocks and sediments. *In:* AMEEN, M. S. (ed.) *Fractography: fracture topography as a tool in fracture mechanics and stress analysis* (1995).

Cox, S. F. The application of failure mode diagrams for exploring the roles of fluid pressure and stress states in controlling styles of fracture-controlled permeability enhancement in faults and shear zones. *Geofluids,* 10**,** 217-233 (2010).

Davidson, J., Siratovich, P., Wallis, I., Gravley, D. and Mcnamara, D. Quantifying the stress distribution at the Rotokawa geothermal field, New Zealand. *New Zealand Geothermal Workshop.* Auckland (2012).

Hoek, E. Fracture of anisotropic rock. Journal of South African Institute of mining and metallurgy, 64**,** 501-518 (1964).

Hudson, J. A. and Harrison, J. P. Engineering rock mechanics - An introduction to the principles, Oxford, Pergamon (1997).

Irvine, R. J. and Smith, M. J. Geophysical exploration for epithermal gold deposits. *Journal of Geochemical Exploration,* 36**,** 375-412 (1990).

Jackson, R., Gorski, B. and Gyenge, M. Geotechnical Properties of Rock: A Data Base of Physical Properties of Canadian Rock Including Both Intact and Residual Strengths. Canada Communication Group - Publishing (1995).

Jébrak, M. Hydrothermal breccias in vein-type ore deposits: A review of mechanisms, morphology and size distribution. *Ore Geology Reviews*, 12, 111-134 (1997).

Ladeira, F. L. and Price, N. J. Relationship between fracture spacing and bed thickness. *Journal of Structural Geology,* 3**,** 179-183 (1981).

MacNamara, P. M. Whangamata area, MPW 27259, Hauraki district, New Zealand. Pacminex NZ Ltd. Ministry of Economic Development, Wellington, unpublished open-file mineral report MR3135 (1972).

Maxwell, M. Report on the geology and mineralisation of Whangamata EL 33062, Coromandel. Gold Mines of NZ Ltd. Ministry of Economic Development, Wellington, unpublished open-file mineral report MR3135 (1980).

Nova, R. and Zaninetti, A. An investigation into the tensile behaviour of a schistose rock. *International Journal of Rock Mechanics and Mining Sciences and Geomechanics Abstracts,* 27**,** 231-242 (1990).

Rabone, S. D. C. Residual total force magnetic anomaly map, Coromandel region. New Zealand Geological Survey Report M183 (1991).

Robson, R. Final technical report on the Onemana prospect, Coromandel Peninsula, NZ PL 31-1956. Ministry of Economic Development, Wellington, unpublished open-file mineral report MR3135 (1992).

Rowland, J. V. and Simmons, S. F. Hydrologic, Magmatic, and Tectonic Controls on Hydrothermal Flow, Taupo Volcanic Zone, New Zealand: Implications for the Formation of Epithermal Vein Deposits. *Economic Geology,* 107**,** 427-457 (2012).

Schöpfer, M. P. J., Arslan, A., Walsh, J. J. and Childs, C. Reconciliation of contrasting theories for fracture spacing in layered rocks. *Journal of Structural Geology,* 33**,** 551-565 (2011).

Sibson, R. H. Brittle failure mode plots for compressional and extensional tectonic regimes. *Journal of Structural Geology,* 20**,** 655-660 (1998).

Sibson, R. H. Fluid involvement in normal faulting. *Journal of Geodynamics,* 29**,** 469-499 (2000).

Sibson, R. H. Seismogenic framework for hydrothermal transport and ore deposition. *In:* RICHARDS, J. P. and TOSDAL, R. M. (eds.) *Structural controls on ore genesis* (2001).

Stevens, M. R. and Boswell, G. B. Geology and Exploration of the Onemana Au-Ag Prospect, Whangamata, Hauraki Goldfield. *In:* Christie, A. B. and Brathwaite, R. L. (eds.) *Australasian Institute of Mining and Metallurgy Monograph 25* (2006).

Vidanovich, P. An aeromagnetic survey over an extinct geothermal system, Onemana, Coromandel Peninsula, New Zealand. Proceedings of the 25th annual conference, New Zealand Branch of the Australasian Institute of Mining and Metallurgy, 1991. 222-224 (1991).

Vidanovich, P. Onemana resistivity trend analysis. Ministry of Economic Development, Wellington, unpublished open-file mineral report MR3856 (1995).

Zuquim, M. P. S., Rowland, J. V., Mauk, J. L., Theron, R. and Atkinson, P. Structural controls on the localisation of Au-Ag epithermal deposits within the Karangahake-Ohui structural trend, Hauraki Goldfield, New Zealand. Proceedings of the 2013 annual conference, New Zealand Branch of the Australasian Institute of Mining and Metallurgy, 2013. In press.